Experimental Characterisation of the Wake of a Bottom-Mounted Two Tandem of Cylinders Placed in a High Velocity Area

A. Santa Cruz, T. Combret, F. Hadri and S. Guillou

Abstract— **Following the development of renewable marine energies, the characterisation of areas with strong marine currents has become necessary. The Normandy coasts (France) are among the sites suitable for the installation of tidal turbine parks because they have significant energy potential. Projects to install machines in these sites raise questions about various factors affecting the performance of the turbines that would be placed there.**

Some current work deals with the understanding of the mechanisms leading to the generation of ambient flow turbulence on the seabed. A particular interest is focused on the impact of the complexity of the bathymetry on the organisation of the wake generated. Indeed, in the seabed the structures are not isolated. On the contrary, successions of structures anchored on the funds can be observed, leading to the interaction of a structure with the wake generated upstream by another one structure. The experimental study deals with the characterisation of the flow around a tandem of "long" cylindrical obstacles of a square section (side H). The distance between these two cylinders is equal to 2H.

As expected, in the present study, the modifications of the topology of the mean flow and the distribution of the turbulent kinetic energy can be observed. Indeed, the interaction between the mean recirculation, generated downstream of each obstacle, is shown.

Keywords— **Renewable marine energies, Particle Image Velocimetry (PIV), Roughness, Obstacle with rectangular section, Obstacle placed on the bottom.**

I. Introduction

THE power production performance of tidal turbines depends on the interaction of various factors, in particular, the level of turbulence of the ambient flow. The presence of energetic structures in the incoming flow is strongly linked to the specific bathymetry of the sites of tidal turbine parks. In Europe, a sector with high energy potential, due to strong sea currents, is the Raz-Blanchard, near the Normandy coast. Due to the machine installation projects in this sector, it is necessary to insist on understanding the mechanisms involved in the generation of the turbulent ambient flow, given the high complexity of the bottom's roughness [3]. The bathymetric charts indicate the presence of elevation differences of up to 5 m. The velocity of the currents is around 5 m/s. Also, in situ, the Reynolds number is of the order of $2.5.10^7$.

The presence of vortices, generated by the variation of elevation in the seabed bathymetry, has been treated in the bibliography with experimental and numerical simulation approaches [3, 4]. A simplified model of the roughness of the seabed can be adopted in order to understand the mechanisms of vortex formation in the seabed [5, 6]. The effect of bottom-mounted obstacles on the flow organisation has been studied for different obstacles shapes: cubic short obstacles [5, 7, 8], ribs or long cylinders [9], combined obstacles [10], distribution of obstacles over the bottom [11].

Moreover, the impact of the seabed morphology on turbulence generation has been studied in a strong tidal stream case. LBM-LES simulations performed in the Raz Blanchard area focus on spatial variations of the flow characteristics, the generation of turbulence at specific seabed landforms. Authors observed that seabed landforms of elongated span-wise dimension are identified as potential generators of high TKE [12].

Inhere, generic cylindrical obstacles with rectangular sections are used to simplify the modelling of the bathymetry of the seabed. The state of art in this topic of research reveals that the wakes generated downstream longs cylinders have been studied by a computational fluids dynamics way [13,14,15,16]. The obstacles are placed on the bottom of the study area of the Hydrodynamic Tunnel of the LUSAC laboratory [17] and

This project was partly financially supported by the region Normandie in the framework CPER 2015-2020, MANCHE 2021: Mer-Littoral "Plateformes d'exploitation de ressources marines". It also benefits from the support of the Conseil départamental de la Manche and the Communauté Urbaine de Cherbourg

A. S. C., F. H. and S. G. are now at Laboratoire Universitaire de Sciences Appliquées de Cherbourg (LUSAC), Unicaen, Cherbourg-en-Cotentin, France (e-mail : alina.santa-cruz@unicaen.fr).

F. Hadri is also in the Laboratoire d'Ingénierie des Systèmes de Versailles (LISV), Université de Versailles, Saint-Quentin-en-Yvelines, France.

Digital Object Identifier: https://doi.org/10.36688/ewtec-2023-579

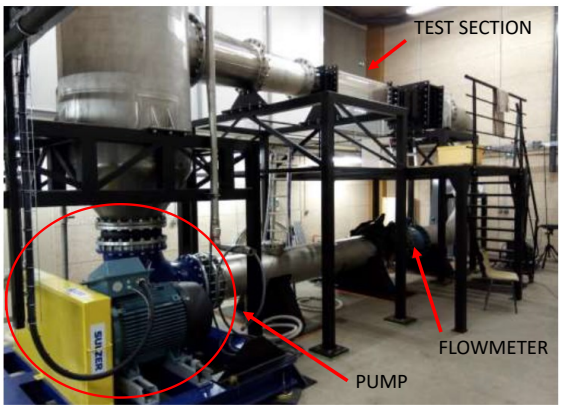

a) The water tunnel is a closed loop. The pump and the electromagnetic flowmeter are placed in the lower branch of the experimental device.

b)

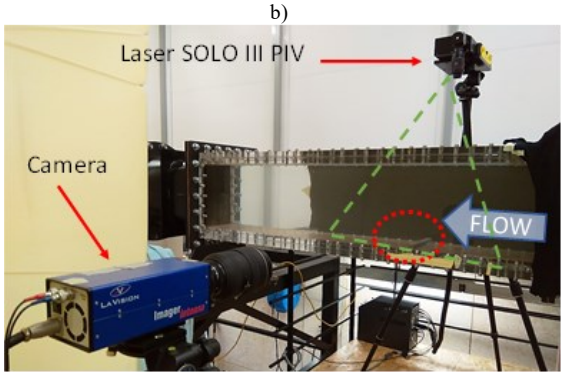

b) The test section: the obstacle is anchored on the bottom. The laser visualization sheet is vertical and the CCD camera is placed perpendicular to the vertical laser visualization sheet. (x, z).

Fig. 1. The LUSAC hydrodynamic water tunnel

occupy its entire width. Measurements are made using Particle Image Velocimetry (PIV-2D) for a velocity flow of 3 m/s.

Previous contributions [1, 2] dealt with the impact of the ratio between the height and the depth of the cross section of the cylinder on the organisation of the near wake. Indeed, the average velocity fields obtained for six different obstacles (with a cross-section aspect ratio varying between 7.5 and 2) highlighted the modification of the organisation of the flow topology. Note that the ratio between the depth and length of the obstacle remains large enough to consider the flow as a “pseudo-2D”. The variation of the cross-section aspect ratio leads to the modification of the topology of the average vortex formation zone, implies the presence of two or even three average recirculation zones in the near wake of the cylinder and leads to the possible presence of a recirculation zone average placed upstream of the cylinder. These first observations opened the door to a more advanced work presented here.

First, the experimental device is described; then near wakes generated downstream the obstacles are presented: a tandem obstacle configuration is compared to a single obstacle one.

II. EXPERIMENTAL DEVICE

The experiments are conducted in the Water Tunnel of the LUSAC laboratory located in Cherbourg-en-Cotentin (Normandy University, France) and the measurements are obtained using Particle Image Velocimetry PIV 2D2C. Figure 1a presents the experimental device, a closed water tunnel. The flow is a loop, and the motion is generated by a helicoidal impeller pump. The measurements are carried out in a test section consisting of 1300 mm long, smooth and transparent Plexiglass square pipeline with 300 mm (W) wide and deep dimensions (cf. Figure 1 b). The water tunnel is provided by an electromagnetic flowmeter.

This experimental study deals with modelling the seabed bathymetry variation impact on the formation of vortices that contribute to the amount of ambient flow turbulence. In a simplified approach, generic cylindrical long obstacles are used. Their cross-section is rectangular, and anchored on the bottom test section (see Figure 2). These obstacles occupy the test section’s width between the two vertical walls. H, the height of the obstacle cross-section, is oriented along the z-axis; its depth (D=H) is oriented along the x-axis, in other words, the flow direction; the y-axis is oriented perpendicular to the obstacle cross-section. The x-origin is set at the front of the obstacle mid-span, and z=0 corresponds to the bottom.

This study is focused on the presence of a tandem of similar obstacles of square section of side H=20 mm and a cross-sectional aspect ratio of 15. The spacing between both obstacles is equal to 2H. As mentioned previously, the ratio W/H impacts the two-dimensionality of the flow generated downstream of the obstacle, particularly in the vicinity of the midspan plane. The threshold of 10, according to the literature [14], makes it possible to differentiate the so-called "long" cylinders from the "short" squared section cylinders.

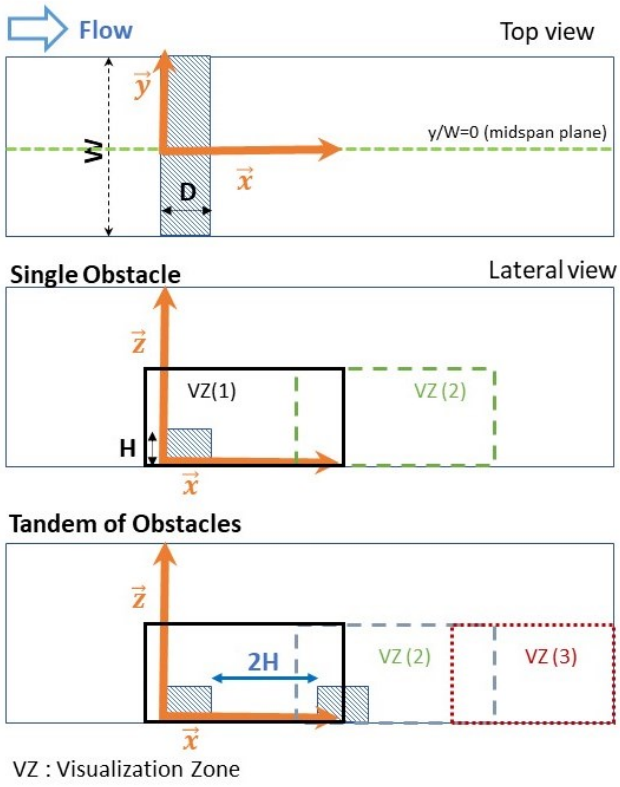

Fig. 2. Simplified model of the seabed roughness and visualization zones.

The values x* and z* (dimensionless) are obtained through the ratio with H: x*=x/H and z*=z/H. For this investigation, the incoming flow (U∞) is equal to 3,3 m/s and the Reynolds Number based on the obstacle height, H, is $Re_H = \frac{U_\infty H}{\upsilon}$, of 65500, with ν the kinematic viscosity of the water.

TABLE I
DESCRIPTION OF THE OBSTACLES, LENGTH OF THE MEAN VORTEX FORMATION ZONE AND POSITION OF THE MEAN RECIRCULATION ZONES CORES.

	Single Obstacle	Tandem of Obstacles
H=D [mm]	20	20
W[mm]	300	300
H/D	1	1
W/H	15	15
LR/H	10	10.3
Coordinates of T1 (T1′)	(x*;z*) =(6.2 ; 1.1)	(x*;z*) =(6.1 ; 1)
Coordinates of T2 (T2′)	(x*; z*) =(2.6 ; 0.5)	(x*; z*) =(2.3 ; 0.5)
Coordinates of T3 (T3′)		(x*; z*) =(2.2 ; 1.3)

To characterize the flow, the measurements are conducted using Particle Image Velocimetry in the mid-spanwise plane. The PIV commercial software used is DAVIS 10 (LaVision) in the plane 2D2C version. The water is seeded with borosilicate glass micro particles with 9-13 µm, with a density close to that of water. The particles are illuminated by a laser Nd: YAG (SOLO-PIV), and the double image acquisitions are made with 5 Hz frequency and a spatial resolution of 1376 $pixels$ × 1040 $pixels$. Statistical calculations were carried out on 1500 instantaneous velocity fields for each case studied.

III. RESULTS

The following section presents results relating to the exploration of the main patterns of the vortex formation zone extracted from the mean velocity fields. Initially, this study focuses on the obstacle within a square cross-section (H=D). In fact, this configuration is the one usually encountered in the literature. The results obtained for the tandem obstacles will be presented a second time. To explore the entire average vortex formation zone, from the obstacle to the point of reattachment of the flow, in the single obstacle case, it is necessary to characterize two neighbouring visualizations zones and concatenate them. In the case of the tandem of obstacles, it is mandatory to lengthen the exploration zone by increasing the number of visualization zones.

A. *Wake flow characterisation for the single obstacle*

Figure 3 presents instantaneous velocity fields for the single obstacle (midspan plane). The vortex formation zone, placed downstream the obstacle can be observed. Particularly the appearance of the vortices at the top of the obstacle, as well as their evolution in the wake, can be shown. A clear separation of the flow is also observed. Indeed, the return flow also generates vortices on the bottom. The distance between eddies escaping from the top and those moving on the bottom being small, their interaction leads to their stretching and to their fusions. Small vortices appear intermittently at the foot of the upstream obstacle front.

B. *Mean flow and turbulence characterisation for the single obstacle*

Figures 3e and 3f show the single obstacle's mean velocity and vorticity fields. As expected from the observations previously made for instantaneous fields, a separation line drawn for $\frac{u}{U_\infty} = 1$ between the free flow and the wake is clearly marked (see Figure 3e). It originates downstream the leading edge of the obstacle and its angle is about 40°. The vorticity along the y axis shown in Figure 3f highlights two counter-rotating zones: a red plume originating at the top of the obstacle indicates the generation of vortices resulting from the shear caused by the contact of the incident flow with the obstacle. Downstream of the obstacle, there is a second zone with an opposite sign.

The length of the mean vortex formation zone, in other words, the distance between the obstacle and the attachment point (abscissa x_R), is defined as $L_R = x_R - D/2$, is equal to $L_R/D=10$. Between the obstacle and the attachment point, there are two average recirculation zones ((T1) and (T2)) (Figure 3e). (T1) is large, originates at the obstacle top

and spreads out along the wake. Note that near the obstacle, it is elongated and follows the shape of the line of separation. Further, in the near wake, its recirculation interacts with the bottom and generates a counter-current flow, giving rise to the appearance of (T2) a counter-rotating recirculation zone. (T2) is smaller than (T1), elongated in shape, and it is blocked between (T1) and the downstream face of the obstacle.

Figure 4a shows the dimensionless longitudinal velocity profiles (along z*). Their shape reveals the presence of the velocity deficit in the disturbed zone compared to the free flow. At x* =2.15, the sign of u/U_∞ changes two times along z* is the footprint of the two mean recirculation zone. At x*=5.15, there's no more a change of sign close to the z*=0, because at this abscissa T1 occupies all the vortex formation zone height. The Turbulent Kinetic Energy (TKE) profiles (Figure 4b) with $k = 3/4(R_{xx} + R_{zz})$ show the increase of the TKE in the near wake of the obstacle[1]. TKE reaches a maximum, of nearly 1 *[m²/s²]*, around the separation line of the mean formation zone. The corresponding turbulence intensity, calculated by using the formula $It[\%] = \sqrt{\frac{k}{{U_\infty}^2}}$, is nearly 30%. A characterization of the vertical evolution of the three-dimensional turbulence made, with acoustic Doppler current profilers, in the eastern part of the Raz-Blanchard site (France) [18] revealed a turbulence intensity of 20% at 7 meters above the bottom. Complementary results obtained from a Large Eddy Simulation (LES) model, implemented in TELEMAC [19], show that, in this tidal energy project site, at the neighbouring of the bottom, the turbulence intensity increases and reaches 30%. This value is similar to the one obtained in the present work.

By comparing the topology of the mean velocity field previously described to results measured on the planes y/W=+/-1/4 (not shown here), it can be concluded that the flow is "pseudo-2D" over the length of the obstacle. In other words, there is only limited development of transverse component velocity allowing the flow to laterally escape.

[1] $R_{xx} = \frac{1}{N-1}\sum_{i=1}^{N} u_i' . u_i'$ and R_{zz} are the Reynolds stresses. The standard definition of turbulent kinetic energy corresponds to the following formula: $k = 1/2\left(R_{xx} + R_{yy} + R_{zz}\right)$. However, the measurements have been made by using a PIV-2D2C. Thus, the (y-axis) component is not available. The formula used here is an estimation of the TKE proposed by the Davis 10 software (La Vision) based on the fluctuations of the two components measured.

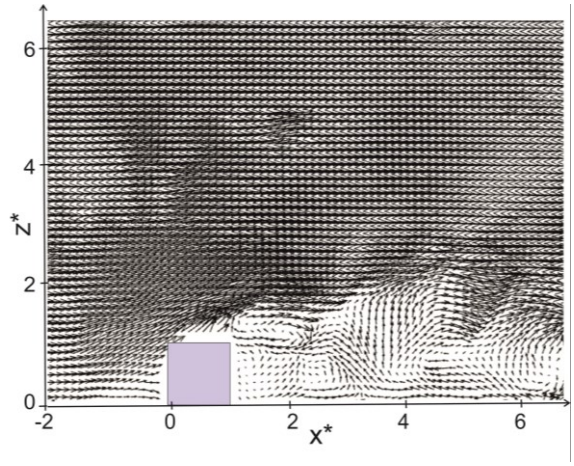

a) Instantaneous velocity field

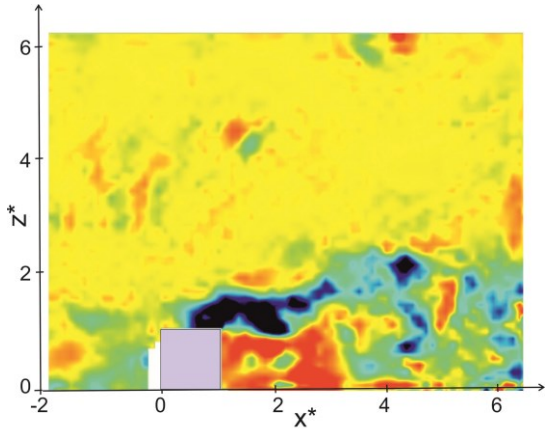

b) Instantaneous vorticity field

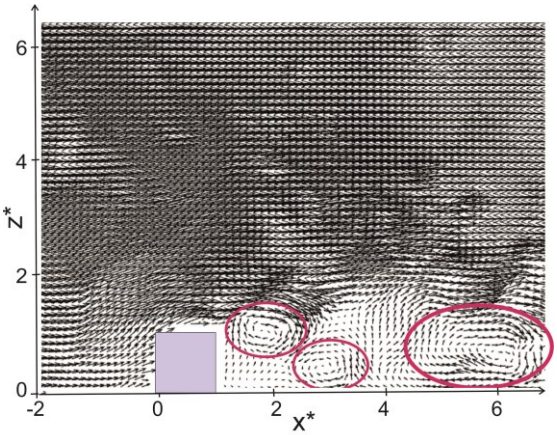

b) Instantaneous velocity field

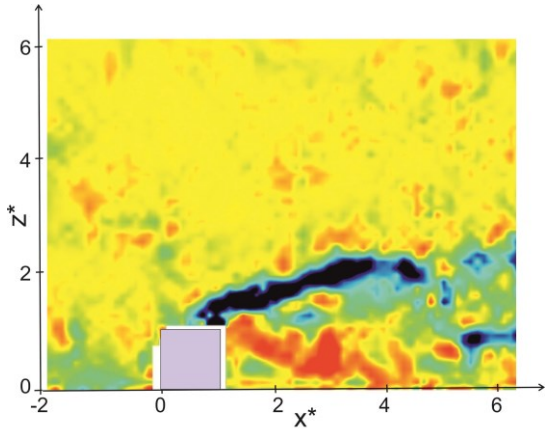

d) Instantaneous vorticity field

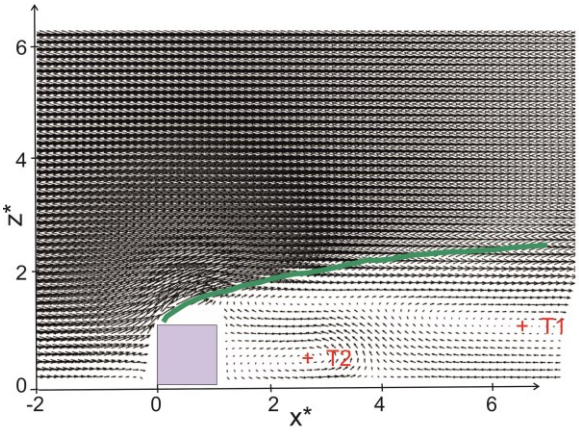

e) Mean velocity field, the green separation line is drawn for u/U∞=1. Coordinates of the core of T1 (x*; z*)=(6,2 ; 1,1) and T2 (x*; z*)=(2,6 ;0,5)

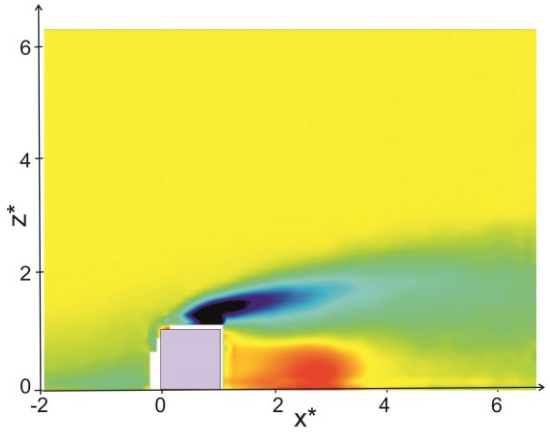

f) Mean vorticity field

Fig. 3. Velocity and vorticity fields - single obstacle

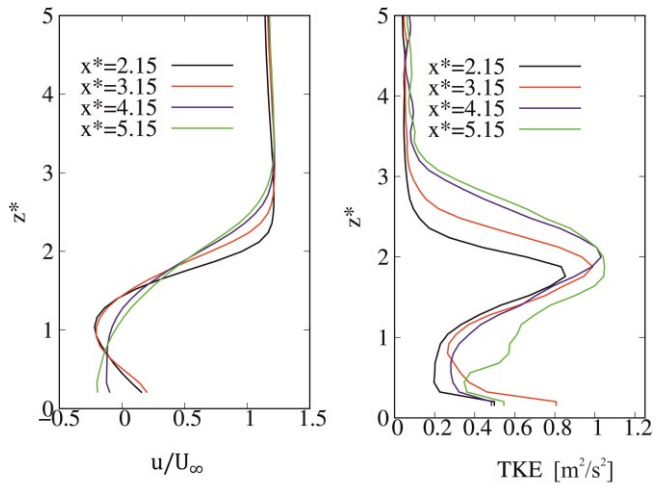

Fig. 4. Dimensionless longitudinal velocity profiles u/U_∞ long z* and TKE profiles along z*

C. *Comparison to the tandem case*

Figures 5a and b respectively show the instantaneous velocity and vorticity fields. As in the case of the single obstacle, the vortices which escape towards the wake are formed at the top of the first obstacle. The vortices are stretched and fragmented from their birth because of the proximity of the top of the second obstacle. Their development is only possible once the second obstacle has been overcome. As previously observed, small slow vortices appear intermittently at the foot of the upstream single obstacle front. In the tandem case, these small vortices seem to be also present. Note that, in previous works (results not noticed in this contribution), for slender single obstacles within a cross-section aspect ratio H/D greater than 1, a small averaged recirculation zone appears at the foot of the upstream single obstacle front [20].

About the topology of the mean vortex formation zone, figures 3e and 5c show that the detachment (on the top of the upstream obstacle, in the tandem case) and the attachment point (at xR abscissa) are nearly at the same places in both studied cases. Consequently, despite the adjunction of the second obstacle, the length of the mean vortex formation zones stays nearly the same as in the single obstacle case (cf. Table 1). The curvature of both separation lines ($\frac{u}{U_\infty} = 1$) has different shapes. However, the topology of the mean vortex formation zone differs. Indeed, in the tandem case, the number of averaged recirculation zones is 4 compared to 2 in the single obstacle case. The vortices cores positions are noticed in the table 1.

The averaged recirculation zones, called in the following T1′ and T2′ (see Figure 5 c and d), present similarities with T1 and T2 previously described in the single obstacle case. As T2, in the single obstacle case, an averaged recirculation zone T2′, placed close to the downstream front of the first obstacle, occupies the entire gap between both obstacles and rotates in the same direction as T2. However, in this case, its genesis is not linked to the existence of a counter-current flow on the bottom, but to the interaction of the shear layer due to the separation between the free flow and the near wake and the blockage between both obstacles. In the tandem case, a main large averaged circulation zone T1′ is also observed. The core positions of T1 and T1′ (see Table 1) are nearly the same ((x*; z*) = (6.1; 1.2) for T1′). However, the area occupied by T1′ is smaller because the presence of the downstream obstacle limits the spreading out of vortices during their shedding. Moreover, the presence of the second obstacle also influences the shape of this main averaged recirculation zone. Indeed, the sheared surface, at the level of the separation line, is constrained by the top of the second obstacle, generating the appearance of an additional average recirculation zone T3'. In a previous contribution [1] an apparent split of T1 into two parts (T1' and T3') has been observed for an obstacle within a cross-section aspect ratio of 0.5 (results not presented here).

Figures 6a and b respectively present the u/U_∞ and TKE profiles (along z*). As expected, for both cases studied, the evolution of the profiles at x* =~2 and x*=~5 have similar shapes.

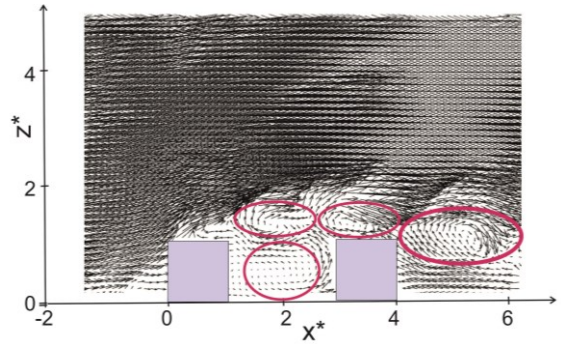

a) Instantaneous velocity field

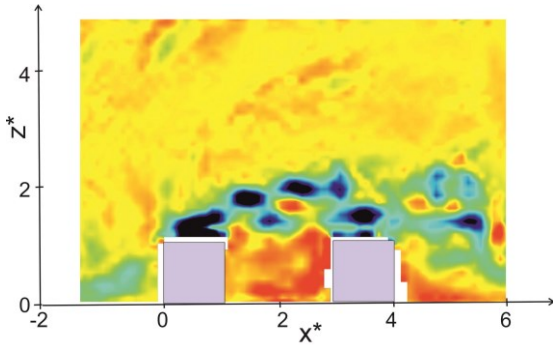

b) Instantaneous vorticity field

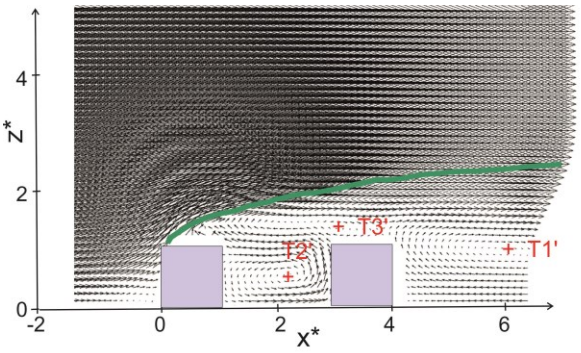

c) Mean velocity field : Coordinates of the core of T1 (x*; z*) = (6,2 ; 1,1) and T2 (x*; z*) = (2,6 ; 0,5)

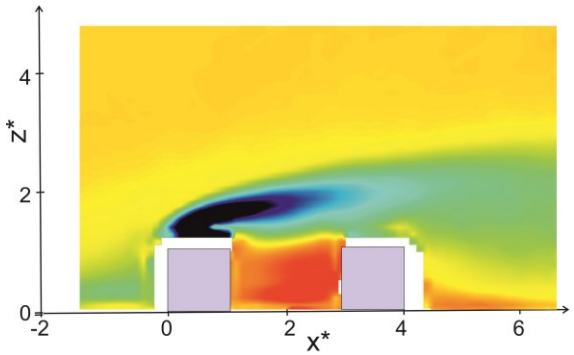

d) Mean vorticity field

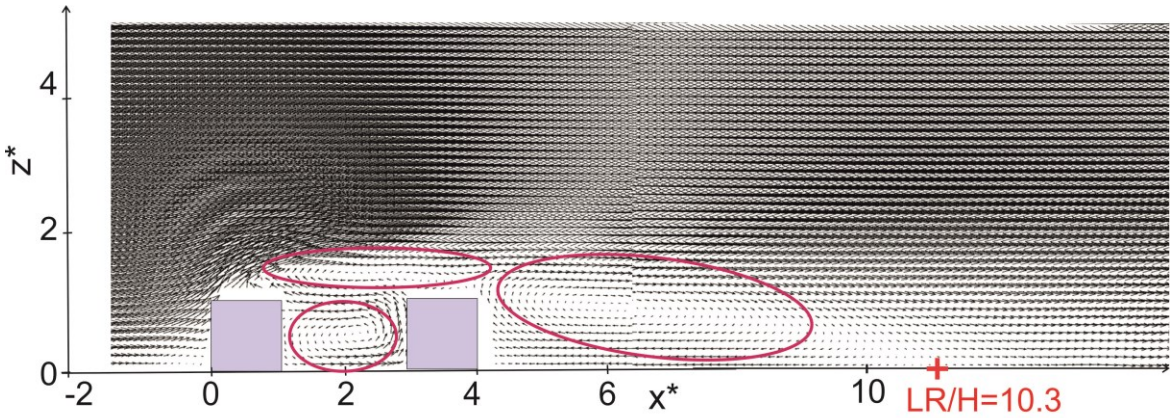

e) Mean velocity field - whole view

Fig. 5. Velocity and vorticity fields – tandem of obstacles

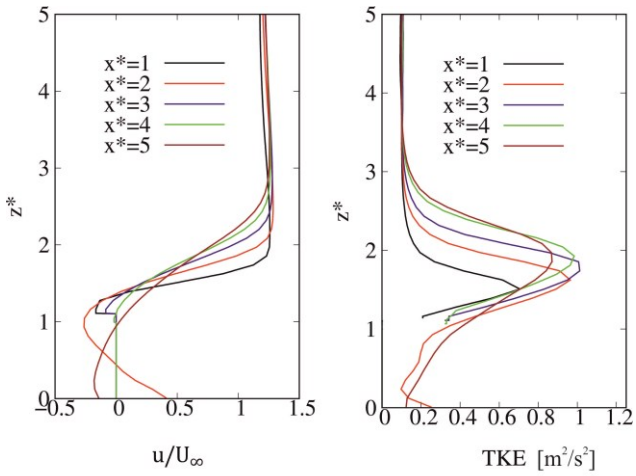

Fig. 6. Dimensionless longitudinal velocity profiles u/U_∞ along z* and TKE profiles along z*.

IV. Conclusion

This work deals with the generation of turbulence resulting from the seabed characterized by its complexity. The variations in the bathymetric elevations are modelled by long cylinders of square sections. In particular, in this contribution, a simple configuration, a cylinder of square section, is compared to a tandem of obstacles.

The results obtained for the single obstacle highlight the birth of the vortices at the top of the obstacle, their spreading out during their displacement in the near wake, and the appearance of counter-rotating vortices that rise, on the bottom, against the current towards the obstacle.

The presence of a second obstacle anchored downstream the first one, with a gap of 2H, leads to modifications of the topology of the vortex formation zone. The number and size of the average recirculation zones downstream of the obstacle vary. In particular, the existence of an additional recirculation zone is observed in the case of the tandem of obstacles. However, it was also noticed that the length of the mean vortex formation zone is nearly the same in both cases. It was also observed that the organisation of the topology into the vortex formation zone presents some similarities. Indeed, the core of the two main averaged recirculation zone have the same position in both cases. As previously observed, complex bathymetry leads to a significant variation in turbulence level. This factor is expected to have a non-negligible impact on available energy captured by a turbine and also its wear.

In the following, our objective is to evaluate the impact of the gap between both obstacles by varying this parameter. In addition, improving spatial and temporal resolutions could lead to a more precise characterisation of the vortex formation and their shedding. Finally, the identification of vortices and the monitoring of the position of their cores is a way to be developed.

References

[1] A. Santa Cruz, F. Hadri, C. Mignonnet and S. Guillou. Impact d'un fond complexe sur la génération de structures tourbillonnaires en zone à haute vitesse. Actes du 25ème Congrès Français de Mécanique, Nantes, 2022.

[2] R. Martinuzzi, C. Tropea. The flow around surface- mounted, prismatic obstacles placed in a fully developed channel flow, ASME, 115(1): 85–92, 1993.

[3] A. Bourgoin, S. Guillou, J. Thiébot, R. Ata. Turbulence characterization at a tidal energy site using large eddy simulations: case of the Aldernery Race, Philosophical transactions A, 378: 20190499, 2020

[4] P. Mercier, M.Grondeau, S.Guillou, J.Thiebot, E.Poizot. Numerical study of the turbulent eddies generated by the seabed roughness at a tidal power site, Applied Ocean Research, 97, 102082, 2020.

[5] M. Ikhennicheu, G.Germain, P.Druault, B.Gaurier. Experimental study of coherent flow structures past a wall-mounted square cylinder. Ocean Engineering, 182:137-14, 2019.

[6] P. Mercier, M. Ikhennicheu, S.S. Guillou, G. Germain, E. Poizot, M. Grondeau, J. Thiébot, P. Druault. The merging of Kelvin–Helmholtz vortices into large coherent flow structures in a high Reynolds number flow past a wallmounted square cylinder. Ocean Engineering, 204, 107274, 2020

[7] Y. Masip, A. Rivas, A. Bengoechea, R. Antón, G. S. Larraona, J. C. Ramos. Experimental study of the turbulent flow around a single wall-mounted prism obstacle placed in a cross-flow and an impinging jet. Advances in Fluid Mechanics, VIII. WIT Transactions on Engineering Sciences, 69: 569 – 584, 2010.

[8] R. J. Hearst, G. Gomit, B. Ganapathisubramaniy. Effect of turbulence on the wake of a wall-mounted cube. Journal of Fluids of Mechanics, 804: 513 - 530, 2016

[9] P. K. Panigrahi, S. Acharya. The Flow Over a Surface Mounted Rib Turbulator Under Single-Mode and Dual-Mode Excitation, J. Wind Engg. Ind. Aerodyn., 92: 1219-1244, 2004.

[10] M. Magnier, P. Druault, G. Germain. Experimental investigation of upstream cube effects on the wake of a wall-mounted cylinder: Wake rising reduction, TKE budget and flow organization. European Journal of Mechanics / B Fluids, 87: 92–102, 2021.

[11] E. Florens, O. Eiff, F. Moulin. Defining the roughness sublayer and its turbulence statistics. Exp Fluids, 54:1500, 2013. URL http://dx.doi.org/10.1007/s00348-013-1500-z.

[12] P. Mercier, S.S. Guillou. The impact of the seabed morphology on turbulence generation in a strong tidal stream. Physics of Fluids, 33, 055125, 2021

[13] Y.Z. Liu, F. Ke, H.J Sung. Unsteady separated and reattaching turbulent flow over a two-dimensional square rib, Journal of fluids and structures, 24: 366 – 381, 2008.

[14] Gu, J. Yang, M. Liu. Study on the instability in separating-reattaching flow over a surface mounted rib, International Journal of Computational Fluid Dynamics, 1029-0257, 2017

[15] F. Zhao, G. Yin, M.C. Ong. Numerical study on flow around a partially buried two-dimensional ribs at high Reynolds number. Ocean engineering, 198, 106988, 2020.

[16] G. Yin, M. C. Ong. Numerical analysis on flow around a wall-mounted square structure using dynamic mode decomposition, Ocean engineering, 223, 108647, 2021.

[17] M. Régniez, M.A.J. Alawieh, J.M. Sanchez, A. Santa Cruz, V. Millet, S. Guillou, F. Chevalier. Caractérisation Vibro-Acoustique D'une Veine Hydrodynamique. Actes du 17èmes Journées de l'Hydrodynamique (JH2020), Caen, 2020.

[18] M. Thiébaut, JF., Filipot, C. Maisondieu, G. Damblans, C. Jochum, L.F. Kilcher, S.S.Guillou. Characterization of the vertical evolution of the 3D turbulence for fatigue design of tidal turbines. Phil. Trans. R. Soc. A 378: 20190495, 2020.

[19] S. Guillou, A. Bourgoin, J. Thiébot, R. Ata. On the spatial variability of the flow characteristics at a Tidal energy site: Case of the Raz Blanchard, Proceedings of the 14th European Wave and Tidal Energy Conference, Plymouth, 2021.

[20] T. Combret, A. Santa Cruz, F. Hadri, and S. Guillou. Etude expérimentale de l'écoulement généré par un obstacle de fond en zone à haute vitesse. Actes du 18è Journée de l'Hydrodynamique, Poitiers, 2022.